CREW EXPLORATION VEHICLE ASCENT ABORT COVERAGE ANALYSIS

**Marc J. Abadie[*], Jon S. Berndt[†], Laura M. Burke[‡], Robert D. Falck[§],
John W. Gowan, Jr.[**], Jennifer M. Madsen[††]**

An important element in the design of NASA's Crew Exploration Vehicle (CEV) is the consideration given to crew safety during various ascent phase failure scenarios. To help ensure crew safety during this critical and dynamic flight phase, the CEV requirements specify that an abort capability must be continuously available from lift-off through orbit insertion. To address this requirement, various CEV ascent abort modes are analyzed using 3-DOF (Degree Of Freedom) and 6-DOF simulations. The analysis involves an evaluation of the feasibility and survivability of each abort mode and an assessment of the abort mode coverage using the current baseline vehicle design. Factors such as abort system performance, crew load limits, thermal environments, crew recovery, and vehicle element disposal are investigated to determine if the current vehicle requirements are appropriate and achievable. Sensitivity studies and design trades are also completed so that more informed decisions can be made regarding the vehicle design. An overview of the CEV ascent abort modes is presented along with the driving requirements for abort scenarios. The results of the analysis completed as part of the requirements validation process are then discussed. Finally, the conclusions of the study are presented, and future analysis tasks are recommended.

INTRODUCTION

VEHICLE DESCRIPTION

The Crew Launch Vehicle (CLV) shown in Figure 1 is comprised of several elements, some of which are derived from components used in other programs. The specifications listed in this section are current as of October 2006; subsequent updates are expected.

The first stage is an upgraded Space Shuttle Solid Rocket Booster (SRB) featuring an additional (fifth) segment. The five-segment SRB is 157.4 feet long, just over eight feet longer than the four-segment Space Shuttle SRB. Thrust at liftoff is about 16% higher than that of the Space Shuttle SRB. This stage burns for about 130 seconds. An interstage structure connects the first and second stages, and features a reaction control system (RCS) to provide roll control during first stage flight and 3-axis rate damping after upper stage cut-off.
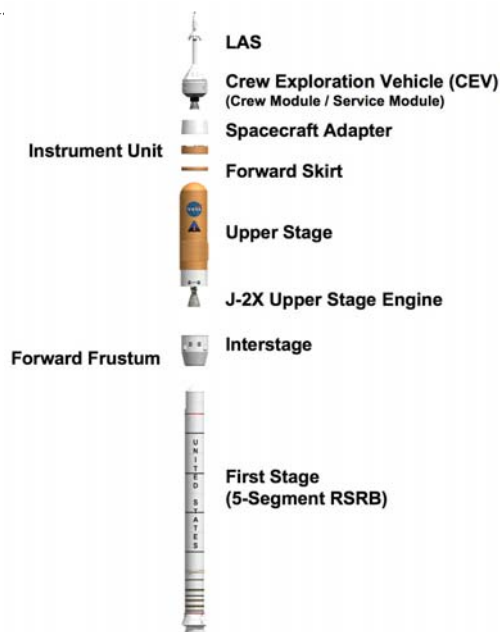

Figure 1: CEV / CLV Diagram

[*] Ascent ARD Support Officer and Former Ascent Analyst, NASA Johnson Space Center, Mailstop: DM3, 2101 NASA Parkway Houston, TX 77058.

[†] Engineering and Science Contract Group (ESCG) Engineer, Jacobs Sverdrup, 2224 Bay Area Blvd., Houston, TX, 77058.

[‡] JobTitle, NASA Glenn Research Center, Address.

[§] JobTitle, NASA Glenn Research Center, Address.

[**] Ascent Analyst, NASA Johnson Space Center, Mailstop: DM4, 2101 NASA Parkway Houston, TX 77058.

[††] CEV Ascent Abort GN&C System Manager, NASA Johnson Space Center, Mailstop: EG4, 2101 NASA Parkway Houston, TX 77058.

The upper stage engine is a J-2X expected to provide approximately 274,000 lbs of vacuum thrust for 51.6 degree inclination International Space Station (ISS) missions. The J-2X may be scaled up to 294,000 lbs of vacuum thrust for the lunar missions. This J-2X is a modern derivative of the Apollo-era J-2 engine used in the second and third stages of the Saturn V. The upper stage structure, constructed with aluminum-lithium alloy, is 87.8 feet long, and 18 feet in diameter, and contains the LH2 and LOX tanks. The upper stage engine is air-started at about 200,000 feet, and nominally burns for over 7 minutes. Above the upper stage are an instrument unit and a spacecraft adapter for the CEV.

The payload is the Crew Exploration Vehicle (Orion), comprised of the Service Module (SM) and the Crew Module (CM). A Launch Abort System (LAS) is attached to the CM until it is jettisoned in second stage. The total vehicle length is about 321 feet, and the weight at liftoff is about 2 million lbs.

ABORT MODE OVERVIEW

The reason for an ascent abort falls into one of three general categories: (1) a partial or total loss of vehicle propulsion, (2) a loss of vehicle control, or (3) a CEV systems failure which results in the inability to achieve orbit. Several abort modes are required to encompass the velocity, altitude, atmospheric, and vehicle configuration changes that occur during ascent. These modes provide abort coverage extending from the launch pad until the CEV achieves a sustainable orbit.

Mode I aborts, also referred to as Launch Abort System (LAS) Aborts, are performed using the LAS and remain a viable option until the LAS is jettisoned at a pre-designated point in second stage. During Mode 1 aborts, the LAS is used to pull the Crew Module (CM) away from the Crew Launch Vehicle (CLV) and Service Module (SM). Mode I aborts are characterized by high aerodynamic loads induced by low altitude maneuvers and high accelerations caused by the launch escape motor. The analysis for Mode I aborts focuses on the relative motion between the CEV and the launch vehicle for different failure scenarios and on the crew loads that are experienced due to the high acceleration forces.

Mode II aborts, also referred to as Untargeted Abort Splashdowns (UAS), do not utilize the LAS. Instead, the CLV upper stage engine is shut down and the SM reaction control system is used to provide adequate clearance between the launch vehicle and CEV. Once the CEV is sufficiently far away from the launch vehicle, the CM separates from the SM, is maneuvered for re-entry, and descends using parachutes to a safe landing location. For Mode II aborts, the analysis described focuses on the CM splashdown locations and the crew loads experienced during reentry.

Mode III aborts, commonly known as Targeted Abort Landings (TAL), involve late second stage failures where the CEV trajectory is modified via a targeted SM engine burn followed by a guided entry to a landing site. The goal of these trajectory control efforts is to select a landing area that maximizes the chances of crew survival and recovery but protects for crew loads and SM thermal constraints. Due to the thermal environment associated with "drooping" into the atmosphere following an upper stage engine failure, the focus of the Mode III analysis is the droop altitude for various scenarios and the ways in which the droop effect can be minimized.

The last type of abort mode is Mode IV, which is an Abort-To-Orbit (ATO). This mode describes cases where an abort is performed following an early shutdown of the upper stage when the SM has sufficient capability to complete a safe orbit insertion and de-orbit burn. Similar to the TAL aborts, the ATO cases must protect the SM from adverse thermal conditions. For the Mode IV abort, the analysis looks at the amount of propellant (or ΔV) required to achieve a sustainable orbit, and similar to TAL, focuses primarily on the droop effects.

ABORT REQUIREMENTS AND CONSTRAINTS

The driving requirements for the abort coverage subtask are as follows:

a. CV0039: The CEV shall provide abort capability starting on the launch pad with the arming of the Launch Abort System through operations in Low Earth Orbit.

b. CV0042: The CEV Launch Abort System shall provide an axial thrust, as measured at sea level (TBR) and 30 (TBR) degree propellant mean bulk temperature conditions, of not less than 15 (TBR-002-12) times the combined weight of the CM+LAS for a duration of not less than 2 (TBR-002-149) seconds.

c. CV0048: The CEV shall translate from the CLV following separation.

d. CV0049: The CEV shall perform an Earth orbit insertion after being delivered to the mission-specific Earth Ascent Staging Target by the CLV.

e. CV0061: The CEV shall provide automated abort to orbit targeting and maneuvers.

f. CV0449: For ISS crew missions, the CEV shall provide ascent aborts that result in landing outside of the Downrange Abort Exclusion Zone.

g. CV0457: The CEV shall be able to perform all aborts without relying on thrust from the CLV.

3-DOF LATE ASCENT ABORT COVERAGE ANALYSIS

The 3-DOF analysis of late ascent abort scenarios is conducted to determine the impact of thrust-to-weight ratio and abort response time on the feasibility and performance of UAS, TAL, and ATO abort scenarios. The analysis is conducted using the Optimal Trajectories through Implicit Simulation (OTIS 4) trajectory optimization software. The analysis is based on nominal 28.5^o (exploration/lunar) and 51.6^o (ISS) ascent trajectories from CLV Design Analysis Cycle 1, Rev. 2. The results shown here are those for the 51.6^o ascent aborts only. The results for 28.5^o mission are detailed in Reference 1, *CEV RAC-2 TDS-04-012/Subtask 5: Late Ascent Abort Modeling Sensitivities Analysis*.

Ascent trajectories from the bounds of launch windows are also examined to determine the impact of launch windows on abort feasibility and performance. The CEV must be capable of performing an abort during launch such that the crew is guaranteed not to land in the North Atlantic Downrange Abort Exclusion Zone (DAEZ), which extends from 150 nmi east of St. John's, Newfoundland to 150 nmi west of Shannon, Ireland. The thrust-to-weight required to perform an abort while avoiding the DAEZ is the largest anticipated for any CEV mission, and thus drives the sizing of the Orion Main Engine (OME).

UNTARGETED ABORT SPLASHDOWN ENVELOPE ANALYSIS

Abort splashdown envelopes are computed to determine potential recovery locations as a function of abort time. The operational sequence assumed for a UAS abort is as follows:

*   Abort is initiated. The CEV is separated from the upper stage.
*   The CEV coasts to sufficiently clear the upper stage and reorient for SM jettison.
*   The SM is jettisoned, and the CM orients itself for reentry above 300,000 ft.
*   The CM reenters the atmosphere. Crossrange can be controlled with bank angle, which is limited to +/- 90° to prevent the crew from going 'heads-down.'

Figure 2 shows the progression of cross-range envelopes for UAS aborts off the 51.6^o inclination mission trajectory. The evolution of potential splashdown locations as the time of abort initiation is moved later in the ascent is illustrated. The launch window duration for a 51.6^o mission is 20 minutes. If the CM reentry can be controlled with bank, then the potential splashdown corridor can be narrowed to minimize the number of recovery assets needed while still providing adequate response time for crew recovery.
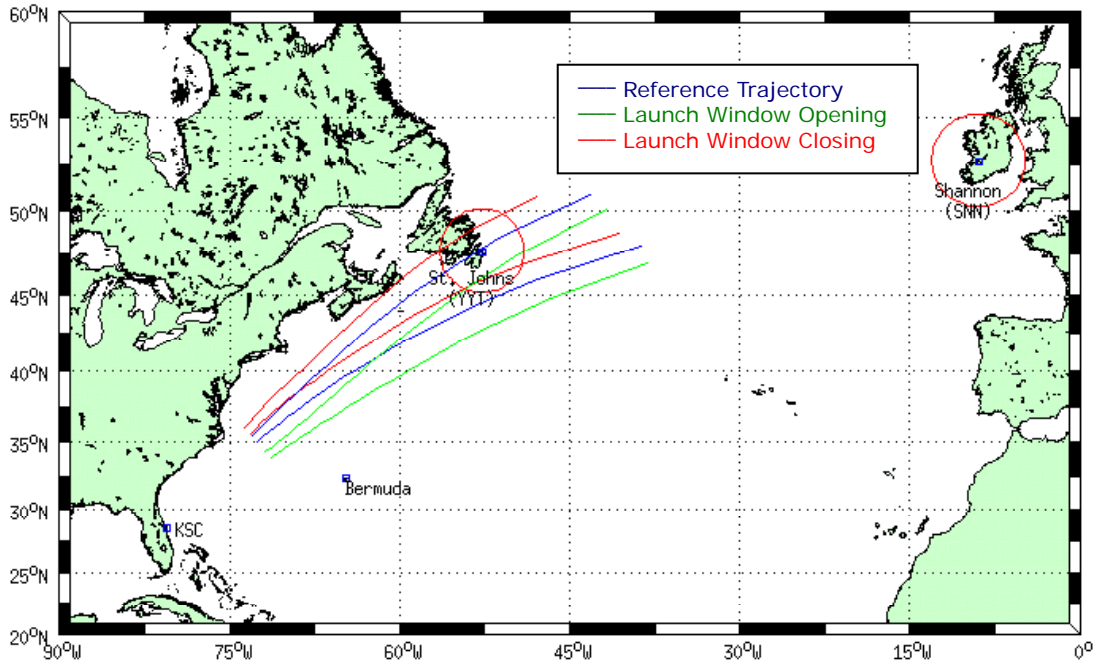
Figure 2: Crossrange Envelopes for 51.6° UAS aborts for 300 through 565 seconds

The data in Table 1 shows when the latest possible Mode II abort to the St. John's recovery area occurs as defined by the DAEZ requirement. The first two rows show the DAEZ entry times for non-propulsive Mode II aborts, which are not referred to as UAS aborts. The ballistic case uses a constant rotation in bank angle to cancel out any effect from the lift vector. The optimal bank reentry type is allowed to move the bank angle through the range of +/- 90°. The ability to control the reentry location with bank effectively allows energy to be removed from the trajectory with bank control, and the CEV thus can land within 150 nmi of St. John's at a somewhat later abort time. Using a banking reentry delays the reentry into the DAEZ by about 1.5 seconds.

Table 1: Latest Possible Mode II Aborts

T/W ratio	Reentry type	Ignition delay (sec)	Latest Mode II abort Time (sec)
0.0	Optimal bank	N/A	560.56
0.0	Ballistic	N/A	559.04
0.2	Optimal bank	15	565.02
0.2	Optimal bank	40	564.04
0.3	Optimal bank	15	566.27
0.3	Optimal bank	40	564.74

TARGETED ABORT LANDING AND ABORT-TO-ORBIT PERFORMANCE ANALYSIS

Targeted abort landings are assessed using the following operational sequence:

- Abort is initiated. The CEV is separated from the upper stage.

- The CEV coasts to sufficiently clear the upper stage and reorient for SM jettison. Coast durations of 15 and 40 seconds are examined to determine the impact of the coast duration on the availability of TAL aborts.
- The CEV performs a main engine burn to loft the vehicle downrange to the landing site while maintaining an altitude of at least 335,000 ft. The altitude constraint is used as an approximation to prevent excess aerodynamic heating until a more integrated analysis can be performed.
- The SM is jettisoned and the CM orients itself for reentry above 300,000 ft. This phase must be at least 40 seconds in duration to provide time for adequate CM/SM separation before reentry.
- The CM reenters the atmosphere. Crossrange can be controlled with bank angle, which is limited to +/- 90° to prevent the crew from going 'heads-down.' The CM is constrained to land within 150 nmi of Shannon, Ireland for an ISS mission abort (or Amilcar Cabral Airport in Cape Verde for an exploration mission abort).

Abort-To-Orbit scenarios are assessed assuming the following operational sequence:

- Abort is initiated. The CEV is separated from the upper stage.
- The CEV coasts to sufficiently clear the upper stage and reorient for SM jettison. Coast durations of 15 and 40 seconds are examined to determine the impact of the coast duration on the availability of ATO aborts.
- The CEV performs a main engine burn to increase vehicle apogee to approximately 100 nmi while maintaining an altitude of at least 335,000 ft. The altitude constraint is used as an approximation to prevent excess aerodynamic heating until a more integrated analysis can be performed
- The CEV coast until it has nearly reached apogee. The exact duration to this phase is controlled by the optimizer.
- The CEV performs a main engine burn to insert into a 100 x 100 nmi orbit.

Analysis indicates that the earliest feasible TAL and the earliest feasible ATO occur at approximately the same time, within one second of each other. For the most part, launch window does not appear to have much of an effect on when TAL and ATO become available. The table below shows the earliest feasible TAL and ATO times for the 51.6^o mission. The earliest feasible aborts for the window closing cases occur substantially later than those for the inplane case. This differs from what is observed in the 28.5^o data. The launch window data is from an older design analysis cycle than the window inplane trajectory, and thus may need to be updated. Table 2 lists the earliest possible TAL and ATO abort capability based on the 3-DOF analysis.

Table 2: Earliest Possible TAL and ATO Aborts

| 51.6^o window inplane | T/W ratio | Initiation coast | |
		15 sec	40 sec
	0.2	562 sec	566 sec
	0.3	552 sec	561 sec

| 51.6^o window opening | | Initiation coast | |
	T/W ratio	15 sec	40 sec
	0.2	**562 sec**	**565 sec**
	0.3	**551 sec**	**560 sec**

| 51.6^o window closing | | Initiation coast | |
	T/W ratio	15 sec	40 sec
	0.2	**568 sec**	**572 sec**
	0.3	**561 sec**	**569 sec**

Coupled with the latest possible UAS abort times from Table 1 above, currently there is an abort coverage gap for non-propulsive UAS aborts except in the T/W = 0.3, 15 second initial coast case. If propulsion can be used to delay the vehicles entry into the DAEZ, then there is only a gap in the T/W = 0.2, 40 second initial coast case. However, the risk associated with performing an OME burn and still having time to prepare for the reentry interface needs to undergo further assessment to determine if this is an acceptable scenario.
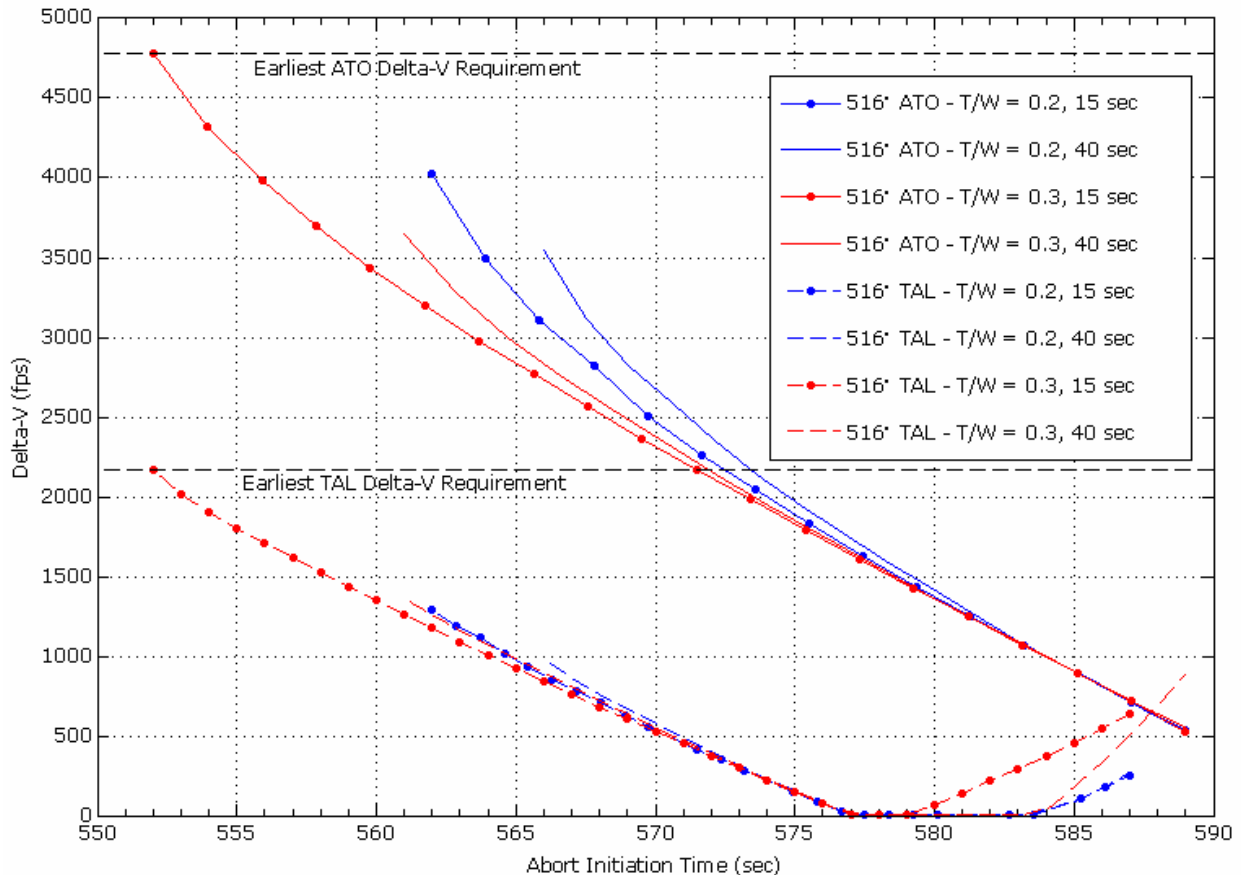
Figure 3: Delta-V vs. Abort Initiation Time for TAL and ATO, 51.6° Inplane Launch

Figure 3 shows the delta-V requirements for TAL and ATO for the 51.6° mission, assuming inplane launch. The TAL delta-V eventually drops to zero, when Shannon can be reached without any propulsion from the service module. It increases again once the CEV has overflown Shannon, since OTIS is attempting a retrograde maneuver to pull the landing point back to Shannon. The left-most point on each curve is the earliest abort that was found for the given thrust-to-weight ratio and ignition delay time. As expected, higher thrust-to-weight ratios and shorter ignition delay times yield earlier aborts. The delta-V required for an ATO is substantially higher than that for TAL. Since the propellant requirement for the 51.6° mission is driven by the abort delta-V, it may be desirable to load the Service Module with enough propellant to accomplish TAL and delay the ATO window until later in the ascent. This would increase the thrust-to-weight of the CEV for a given engine size, and thus move the first feasible abort capability earlier.

6-DOF ASCENT ABORT COVERAGE ANALYSIS

The Architecture for Exploration Studies (ARES) 6-DOF multi-body simulation was utilized to assess each of the four different ascent abort modes. The baseline for the analysis consists of a 51.6° inclination International Space Station (ISS) mission with a nominal ascent trajectory and vehicle configuration based on Design Analysis Cycle (DAC)-0 Rev. 0.

LAS RELATIVE MOTION ANALYSIS

To ensure that a successful LAS abort is achievable, the relative motion between the Launch Abort Vehicle (LAV, i.e., the combined CM and LAS configuration) and the stack (i.e., the entire CLV / CEV configuration minus the LAV) is analyzed for various LAS abort cases. In addition, the assessment also analyzes the relative motion between the CM and the LAS following abort initiation and subsequent LAS jettison. Relative motion for a nominal jettison of the LAS was not explored in this analysis. Five different abort initiation time regions were analyzed as part of this initial study. The LAS abort regions analyzed are as follows: (1) pad abort, (2) abort at maximum LAV separation drag, (3) low altitude (i.e., approximately 30 kft) abort, (4) abort at maximum dynamic pressure (i.e., max-q), and (5) high altitude (i.e., approximately 240 kft) abort. Due to the large number of dispersions that could impact the capability of the LAS and crew survivability, a Monte Carlo analysis was required to gain confidence in the current CEV abort requirements. To analyze the relative motion, the distance between two points, one on each vehicle element, is estimated based on the simulated trajectory of each body. For the relative motion between the LAV and the stack, the two points selected correspond to the midpoints on the central axes of the LAV and the stack. For the relative motion between the CM and the LAS, the midpoints of the CM and LAS were used. To account for the shape of the body and any other limiting factors, a minimum safe distance was assumed. For the relative motion between the LAV and the stack, the minimum safe distance was assumed to be approximately 500 ft. For the CM and LAS relative motion, the safe distance was assumed to be 375 ft. The thrust capability of the LAS is assumed to be equal to 15 times the initial weight of the LAV at the start of the burn. For this initial analysis, the escape motor thrust is held constant for two seconds after abort initiation and then instantaneously reduced back to zero.

The analysis results indicate that adequate separation can be achieved for all of the pad, max drag, and high altitude abort times. However, for certain Monte Carlo cases with the other two abort times, the LAV separates adequately from the stack and then the separation distance decreases below the minimum safe distance a few seconds later. The reduction is separation distance occurs due to the fact that after escape motor burnout, the speed of the LAV drops well below that of the stack, which is continuing to thrust. Since both vehicles are traveling in more or less the same plane, the stack catches up with the LAV. For the low altitude abort time, 93% of the simulation runs drop below the safe distance of 500 ft after LAS burnout. The analysis shows a strong correlation between the offset angle of the escape motor thrust and the reduction in separation distance after LAS burnout. The larger offset angles result in larger pitching moments, which cause the vehicle to turn out of plane and avoid the path of the stack, thereby improving the overall relative motion. A similar phenomenon is observed for the relative motion between the CM and the LAS after LAS jettison. For the max-q abort time, 64% of the runs violate the minimum safe distance of 375 ft due to the reduction in separation distance after LAS burnout. Again, by inducing an out of plane pitching moment, the overall relative motion can be improved.
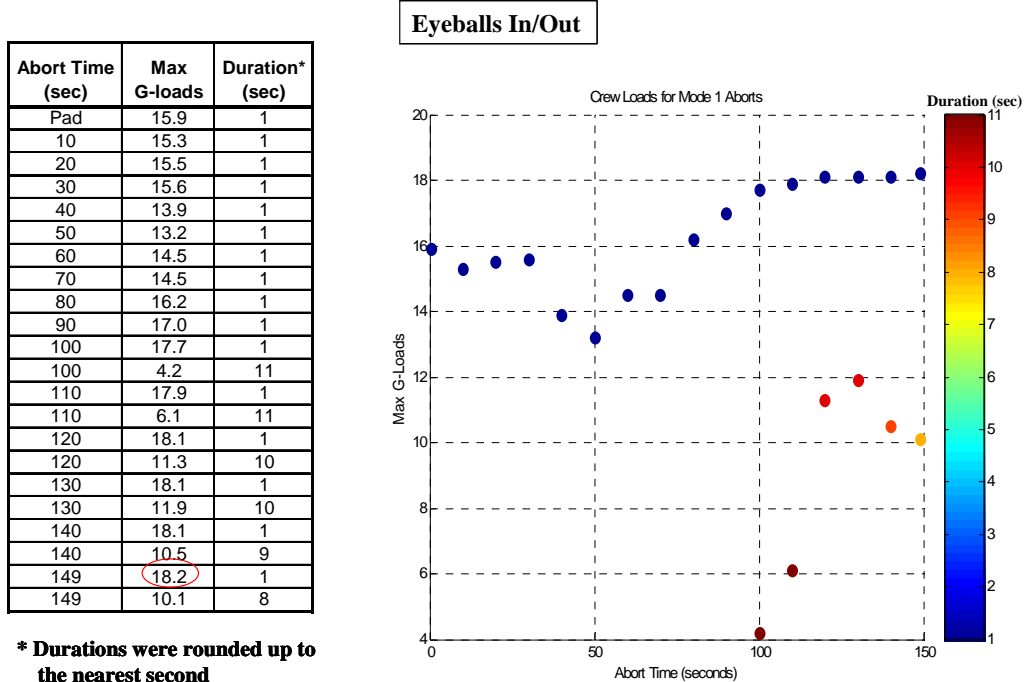
LAS CREW G-LOAD ANALYSIS

With a high thrust LAS escape motor, which is required to escape the potential threat of debris and overpressure caused by first stage failure events, the crew may be exposed to high g-loads during LAS aborts. This study assesses crew loads and vehicle rates during these LAS aborts. At the time of this analysis, the CEV requirements call for a LAS escape motor with a thrust-to-weight ratio equal to 15 (at sea level). As mentioned in the relative motion section, the ARES simulation assumes this same thrust-to-weight. Since the simulation assumes a constant escape motor thrust during the burn, the acceleration can exceed 15 g's as the weight of the vehicle is reduced due to the loss of propellant. Also, the assumption that the thrust instantaneously drops to zero following the burn is overly conservative when analyzing crew g-loads. In reality, the escape motor thrust curve will be designed with consideration for g-loads and the thrust will tail-off as the burn nears completion, which will result in a more benign shift from positive to negative g-loads following LAS burnout.

Positive and negative g-loads for all three vehicle seat axes (eyeballs-in/out, left/right, and down/up) are compared against Human System Integration Requirement (HSIR) limits. Also, roll rates and pitch rates for each

case are analyzed and compared with the HSIR constraints. LAS aborts are examined every 10 seconds from 0 seconds to 150 seconds Mission Elapsed Time (MET). LAS abort capability ends with nominal LAS jettison, which is assumed to occur at 150 seconds MET.

When analyzing the acceleration during the LAS abort, two different acceleration peaks are observed. The first peak is due to the LAS escape motor thrust. These accelerations are very high and very brief. The second acceleration peak has a longer duration but does not reach as high a magnitude. These accelerations are caused by the atmospheric reentry of the later aborts that reach a velocity high enough to drive up the loads. The LAS escape motor induces vehicle accelerations resulting in over 18 g's eyeballs-in. The later LAS aborts exhibit slightly higher g-loads due to reduced atmospheric drag effects. However, there are also earlier abort scenarios executed at the higher density, lower altitudes that exhibit a large eyeballs-in g-load immediately followed by a large eyeballs-out load after escape motor burnout. This is most pronounced for abort times near the point of maximum drag.

Figure 4 shows a data reduction of the peak g-loads across the LAS abort window. The duration of each g-load is designated in color per the color range key on the right side of the figure. As the illustration shows, the early peaks caused by the LAS escape motor last for a very brief period of time, less than 1 second. A second set of maximums are shown for aborts at 100 seconds through 149 seconds MET. Again, these represent the smaller, secondary peaks that are caused by atmospheric reentry of the later LAS aborts. These g-load peaks are approximately 10 to 12 g's and last for 8 to 12 seconds in duration.

Abort Time (sec)	Max G-loads	Duration* (sec)
Pad	15.9	1
10	15.3	1
20	15.5	1
30	15.6	1
40	13.9	1
50	13.2	1
60	14.5	1
70	14.5	1
80	16.2	1
90	17.0	1
100	17.7	1
100	4.2	11
110	17.9	1
110	6.1	11
120	18.1	1
120	11.3	10
130	18.1	1
130	11.9	10
140	18.1	1
140	10.5	9
149	18.2	1
149	10.1	8

* Durations were rounded up to the nearest second

Eyeballs In/Out

Figure 4: Maximum X-axis G-loads for Various Abort Times

Also, the plot shows that the maximum total acceleration dips down around 50 seconds MET. This low point on the curve corresponds to the approximate point of maximum dynamic pressure during ascent, thereby reducing the overall acceleration. This time region, however, is also characterized by a relatively large swing from positive to negative g-loads. For an abort at 30 seconds MET, the crew experience approximately 15 g's eyeballs-in, followed by about 10 g's eyeballs-out over a period of several seconds. Again, this extreme g-load shift is overly estimated in this analysis due to the conservative assumptions regarding thrust shaping. However, even with this conservatism, the crew g-loads still remain within HSIR limits. In fact, all LAS test cases are shown to meet the HSIR limits. Finally, the roll and pitch rates are analyzed for all LAS aborts and are within HSIR limits as well.

UAS SPLASHDOWN LOCATION ANALYSIS

This analysis estimates the latest time at which a CLV upper stage engine shutdown (and ensuing UAS abort) can occur and still result in a CM splashdown no further east than a 150 nm radius about St. John's, Newfoundland. The 150 nm range is a limit imposed to allow a timely recovery of the crew with assets based at St. John's before

the cold North Atlantic waters pose a survivability risk. Outside this radius, toward the mid-Atlantic has been termed the Downrange Ascent Exclusion Zone (DAEZ).

The engine failure time is varied from 480 to 550 seconds, at five second intervals. The geodetic latitude and longitudes from the completed ARES simulations were plotted using Google Earth™ (see Figure 4-20). In order to determine the accuracy of Google Earth™ in visually plotting the coordinates, the initial coordinates (representing the launch site) from an ARES data output file were entered, and the location shown and marked corresponded to the launch pad hold-down posts within about 70 ft. The coordinates for St. John's airport were entered and the location shown and marked corresponded to the center of the airfield. Distances from the airport to a splashdown point were determined using a measurement tool within the Google Earth™ application. A cross check was done for the measurement tool, comparing the distance calculated by Google Earth™ with the distance calculated by a great circle calculator. The two distances measured were within 1 nmi of each other.

The results are plotted in Figure 5. Utilizing lift-up entry guidance, an engine shutdown at about 526 seconds results in a splashdown 150 nmi east of St. John's. A set of cases are also run using a ballistic entry mode. In this mode, the capsule rotates slowly, so the lift vector rotates and the net lift is nulled out. For the ballistic case, an engine shutdown at 543 seconds results in splashdown at the 150 nm limit east of St. John's. It should be noted here that further analysis with higher fidelity atmosphere, winds, and propulsion models may significantly change the results.
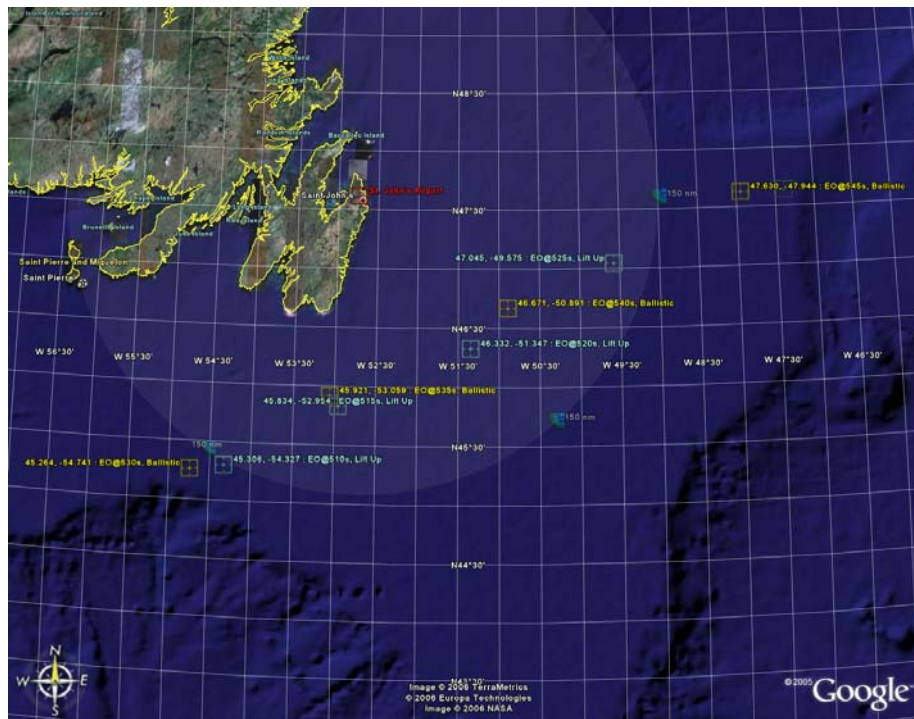

Figure 5: UAS Splashdown Locations

UAS CREW G-LOAD ANALYSIS

In addition to the g-load assessment for LAS aborts, this analysis also assessed crew loads and vehicle rates during UAS aborts. Positive and negative g-loads for all three seat axes (eyeballs in/out, left/right, and down/up) were compared against HSIR limits, as well as the vehicle roll rates and pitch rates. UAS aborts were simulated assuming both lift-up CM reentry and no-lift CM reentry. LAS abort capability ends with nominal LAS jettison at 150 seconds MET. TAL and ATO abort capability picks up around 550 seconds MET. Thus, these times were used to bound the UAS abort test matrix. Originally, aborts every 50 seconds between 150 seconds and 550 seconds were included in the test matrix. However, more cases were added to look deeper at the abort times characterized by high g-loads.

With a CM lift-up reentry attitude, the results show that the eyeballs-in g-loads peak at about 10 g's at 10 seconds duration for aborts around 350 seconds MET due to steep atmospheric reentry. For UAS aborts with a ballistic reentry attitude, the eyeballs-in g-loads peak at around 17 g's at 8 seconds duration for aborts around 450

seconds MET, again due to steep atmospheric reentry. The results clearly show that the crew g-loads can be reduced by employing a guidance scheme that controls lift, as in the lift-up reentry scenario. For both the lift-up and ballistic cases, the Y and Z axes g-loads remain well below HSIR limits, as do the roll and pitch rates for these scenarios.

ATO DROOP ALTITUDE ANALYSIS

The ATO boundary is defined as the earliest CLV upper stage engine failure or abort time where the vehicle can still achieve a safe, sustainable orbit with the SM engine while maintaining an altitude above the minimum droop altitude. For this analysis, the Powered Explicit Guidance (PEG) Linear Terminal Velocity Constraint (LTVC) algorithm, also known as PEG-4, was utilized to perform all SM burns. Although this type of burn is near optimal for propellant usage, it is not necessarily optimal for maximizing the droop altitude and therefore will likely result in an overly conservative (i.e. late) ATO boundary. To determine the abort mode boundary, a range of engine-out (EO) times was simulated at one second intervals from 540 seconds until MECO. The assumptions used for the ATO abort mode analysis are as follows:

1) the minimum droop altitude for ATO aborts is 335 kft,
2) the minimum safe orbit for ATO aborts is 100x100 nm,
3) the SM engine thrust-to-weight (T/W) ratio is approximately 0.2,
4) the maximum ΔV capability of the SM engine is 4700 fps, with 340 fps of that total ΔV reserved for the deorbit burn,
5) a full SM propellant load of 20,500 lbm is baselined, and
6) a 20 second delay time is required in between ATO abort initiation (i.e. separation from the CLV) and SM engine ignition.

A sensitivity analysis was later performed for most of these assumptions to show the variation in the ATO boundary. Since a full SM propellant load is assumed, ATO capability is not constrained by SM ΔV capability, rather it is limited by the minimum droop altitude to protect for SM thermal conditions. Based on a preliminary thermal analysis performed by the NASA Johnson Space Center Aeroscience and Flight Mechanics Division, the minimum droop altitude is estimated to be 335,000 ft.
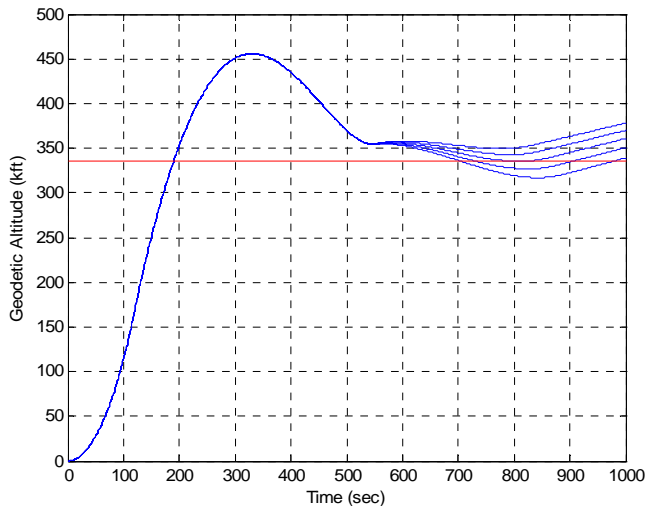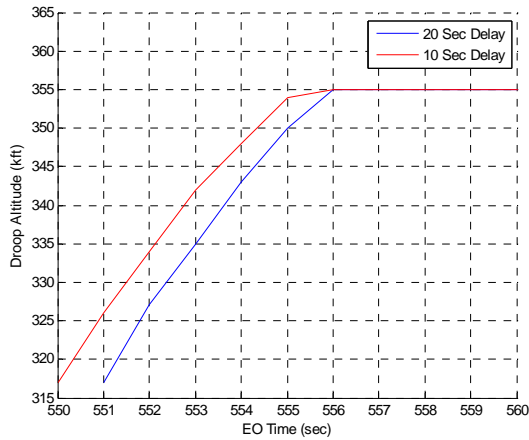

Figure 6: Altitude Profile for EO times from 551–555 sec

Using PEG-4 guidance, the first of two SM burns is simulated in ARES to determine the droop altitude that is reached for various EO times. For the baseline configuration (i.e., employing the configuration and assumptions listed above), the earliest EO time that does not violate the droop constraint is 553 seconds. At this EO time, the point along the trajectory where the droop altitude reaches its minimum is about 250 seconds after abort initiation and occurs prior to SM burn completion. Figure 6 shows the altitude profile for EO times ranging from 551–555 seconds (i.e., 2 seconds before and after the droop constrained ATO boundary).

For an engine failure at 551 seconds, the droop altitude is approximately 317,000 ft. Therefore, even if the droop altitude constraint of 335,000 feet is too conservative and the actual constraint is 20,000 feet lower, ATO 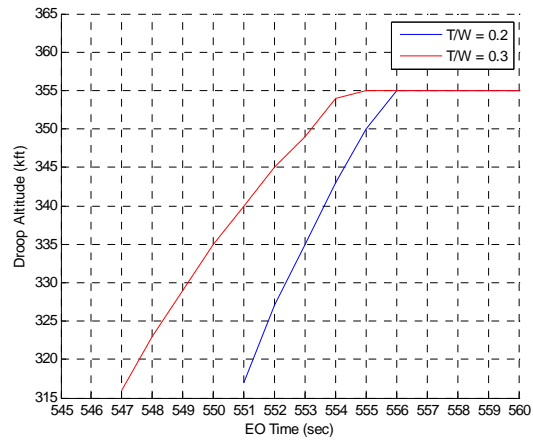capability will only improve by approximately two seconds. Further sensitivity analyses were done for the assumptions regarding T/W ratio, SM ignition delay time, and final orbital altitude. As shown in Figure 7a, the droop altitude and corresponding ATO boundary are improved by about one second by decreasing the SM main engine ignition delay time to ten seconds. Similarly, Figure 7b shows that ATO capability can be achieved about three seconds earlier by using a 0.3 T/W ratio. The final orbital altitude had very little effect on the droop altitude and actually delayed the first ATO capability by a fraction of a second.

(a) Delay Time Sensitivity   (b) T/W Ratio Sensitivity

Figure 7: Droop Altitude v. EO Time

ELEMENT DISPOSAL ANALYSIS

This analysis was conducted to determine how many seconds of abort initiation for UAS, TAL, and ATO aborts result in CLV upper stage disposal over Eurasia for 51.6 degree inclination trajectories. Another way to look at this is to determine what underspeeds result in upper stage disposal over Eurasia. There are a number of off-nominal situations that result in an upper stage disposal issue for CLV. First, if an upper stage engine failure occurs, there is a chance the upper stage will fall short of the nominal disposal zone in the Indian Ocean and possibly impact Eurasia. Also, if the J-2X engine exhibits off-nominal performance producing a large enough underspeed or if there is a reason to manually shutdown the J-2X prematurely, this disposal problem can occur. Finally, significant underspeeds can result from an off-nominal flight day where systems and trajectory dispersions degrade performance and the loaded flight propellant reserve (FPR) is not enough to protect for these dispersions. This study attempts to encompass all of these malfunctions by identifying both the J-2X engine failure times and the underspeeds that result in upper stage impact on Eurasia.

The results show that an upper stage footprint for an abort initiated at 566 seconds begins to impact northwestern Eurasia. Over the next seven seconds, aborts result in upper stage disposal on Eurasia before the footprint shifts into the Indian Ocean as intended for nominal disposal. Figure 8 illustrates the entire range of (intact) upper stage impact points and the corresponding underspeed. A debris footprint will encompass each impact point due to the upper atmospheric breakup of the upper stage. Debris footprints for each of the disposal trajectories were also assessed, and these results can be found in Reference 2. MECO underspeeds between approximately 150 fps and 850 fps result in Eurasia impact. These results have been presented to the Constellation Launch Range Safety Panel and are not expected to be an issue that should affect CLV/CEV design.
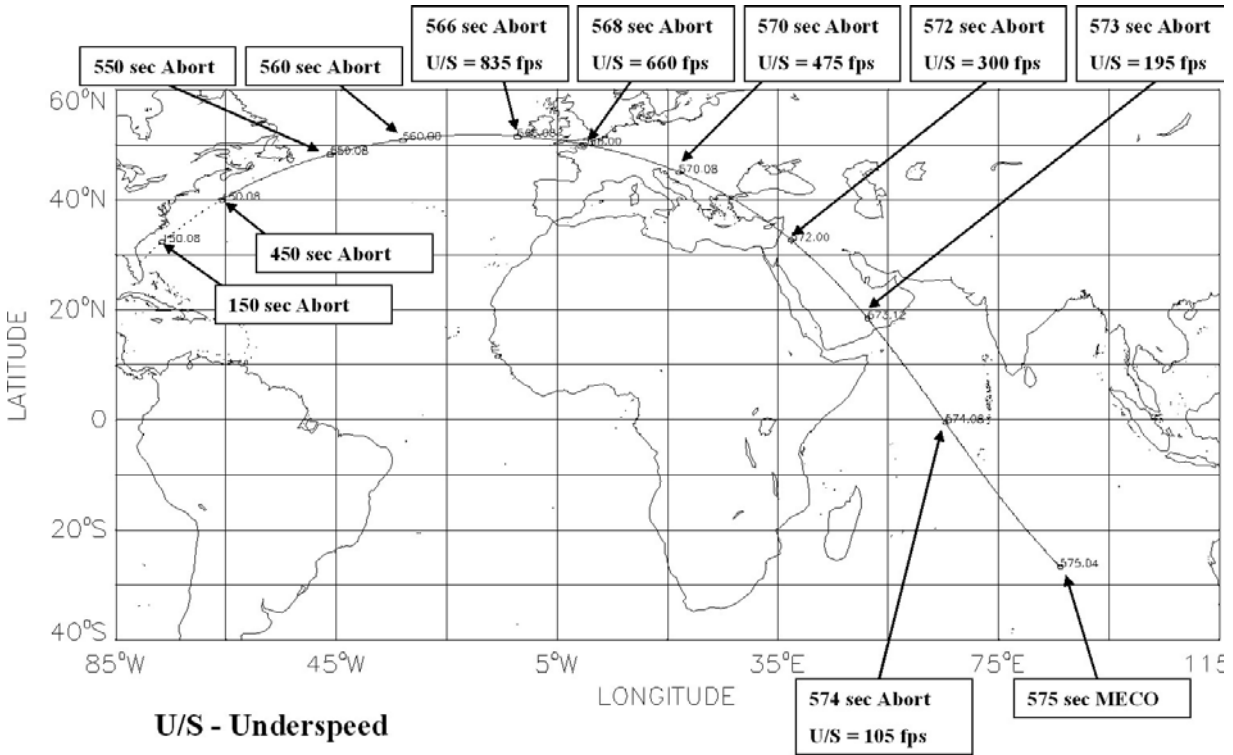
Figure 8: Intact Upper Stage Impact Points for Various Abort Times

ABORT BOUNDARY ESTIMATES

Based on the assumptions listed earlier and the simulation capabilities at the time, preliminary estimates of the abort mode boundaries were obtained. These initial boundary estimates, which indicate where a given abort mode capability is first achieved and when it is no longer viable, are co-plotted with the nominal trajectory altitude profile in Figure 9.
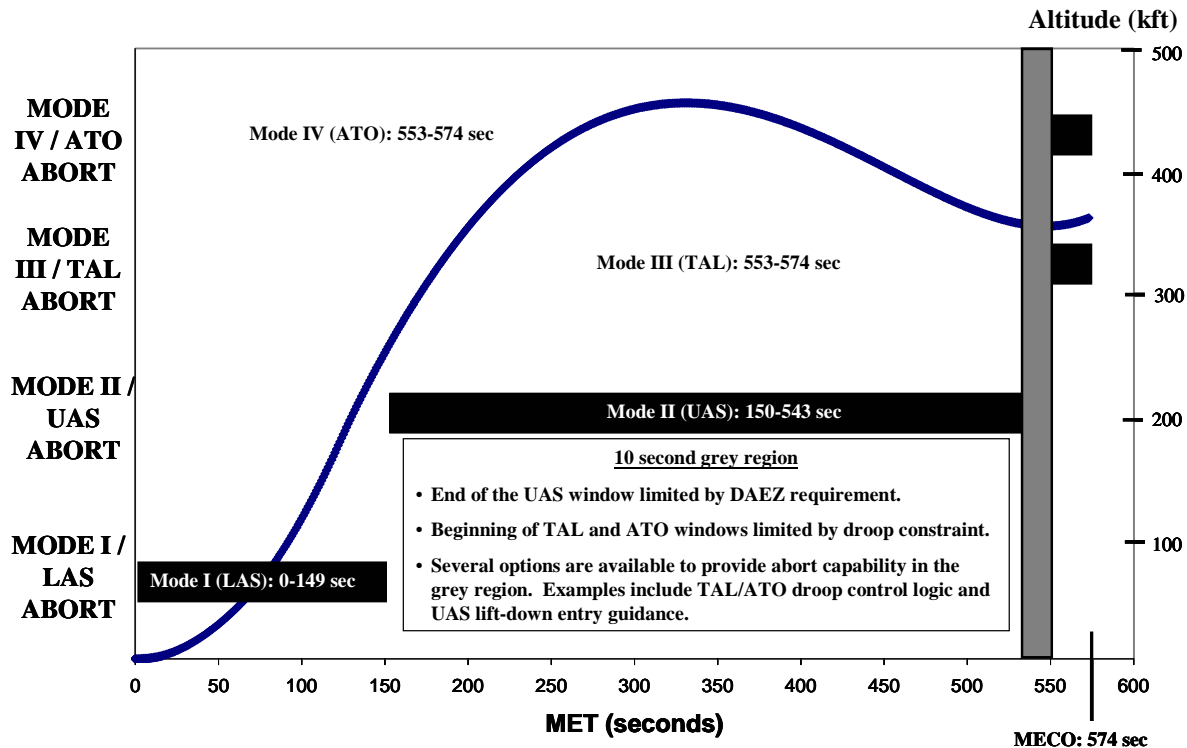
Figure 9: Preliminary Abort Boundaries Based on 6-DOF Analysis

Figure 9 indicates that there is a 10 second gap between the last UAS boundary at 543 seconds and first TAL / ATO capability at 553 seconds. This gap, however, is not expected to be an issue once more sophisticated techniques are employed. The 6-DOF ATO analysis completed to date only analyzed the droop altitudes for SM burn sequences that utilize the PEG-4 guidance algorithm. While PEG-4 likely results in a burn that minimizes delta-V and propellant usage, it is unlikely that this burn sequence optimizes the droop altitude, which has more of an impact on the ATO boundary. The addition of a droop control guidance algorithm is expected to close the entire 10-second gap between UAS and TAL / ATO. The droop control techniques will involve increasing the burn attitude so that the SM engine is firing at some high LVLH pitch attitude to raise the droop altitude. The vehicle may only need to fire the SM engine at the higher pitch attitude for a short period of time before it can then shift to the PEG-4 guidance mode or use some other targeting scheme to begin raising perigee once the droop altitude is no longer a concern. This assumes, however, that SM thermal concerns can be completely mitigated by maintaining an altitude above 335 kft. Some argue that the higher pitch attitude associated with droop control logic may present thermal concerns as well. Other possible methods for closing the gap between UAS and TAL / ATO include CM entry lift control for late UAS aborts, a SM retrograde burn for early TAL aborts, or an offload of SM propellant for all ISS missions. Each of these options has its potential benefits and concerns and will need to be fully analyzed before conclusive statements can be made.

CONCLUSION AND FUTURE WORK

Based on the results of the 3-DOF and 6-DOF analysis of CEV ascent abort coverage for ISS missions, it is anticipated that the CEV design will be able to successfully meet all of the current requirements described in Section 3.0. Furthermore, it does not appear that any changes to the requirements need to be made based on the current data available. Overall, the 6-DOF analysis results have compared relatively well with that of the 3-DOF simulations. Although the 6-DOF analysis completed to date has shown a ten second gap may exist between Mode II and Mode III/IV aborts due to the DAEZ for the ISS mission, the elimination of the gap is not expected to be an issue once the techniques outlined earlier have been implemented. Each of these will be explored to understand the associated benefits to be gained in later UAS aborts and earlier TAL/ATO aborts.

Additionally, further analysis does need to be performed for all abort modes to ensure that the vehicle's capability is being accurately reflected and that the vehicle is protected for realistic failures or dispersions that may

be present during the actual mission. The LAS escape motor thrust curve should be more accurately modeled with an expected profile and the crew g-loads reassessed. Due to the limitations of the ARES simulation, very limited Mode III analysis has been completed to date. Therefore, once the ARES Mode III simulation capabilities are expanded, detailed analysis of this abort mode will need to be performed.

ACKNOWLEDGMENTS

REFERENCES

[1] Falck, R, 2006. *CEV RAC-2 TDS-04-012/Subtask 5:Late Ascent Abort Modeling Sensitivities Analysis, FltDyn-CEV-06-92*. NASA Johnson Space Center, Houston, TX.

[2] Gowan, J., 2006. *CEV RAC-2 TDS-04-012/Subtasks 1 and 4:Integrated Ascent Abort Coverage Analysis, EG-CEV-06-52*. NASA Johnson Space Center, Houston, TX.